

CMS Physics Analysis Summary

Contact: cms-pag-conveners-susy@cern.ch

2016/03/20

Further SUSY Simplified Model interpretations for Moriond 2016

The CMS Collaboration

Abstract

A variety of searches for supersymmetry has been carried out by the CMS collaboration based on the 13 TeV pp collision data collected in 2015. In this note, we present a number of additional interpretations of these searches in different SUSY simplified models, complementing the previous preliminary results.

Contents

| | | |
|-------|--------------------------------|----|
| 1 | Introduction | 2 |
| 2 | Included searches | 2 |
| 2.1 | Hadronic final states searches | 2 |
| 2.2 | Leptonic final states searches | 2 |
| 3 | New interpretations | 3 |
| 3.1 | Gluino induced decays | 4 |
| 3.1.1 | T1tttt | 4 |
| 3.1.2 | T5ttttDM175 and T5ttttDegen | 5 |
| 3.1.3 | T1ttbb | 6 |
| 3.1.4 | T5ttcc | 11 |
| 3.1.5 | T5qqqqWW | 12 |
| 3.2 | Squark induced decays | 14 |
| 3.2.1 | T2qq, T2tt, T2bb | 14 |
| 3.2.2 | T6ttWW | 17 |
| 3.2.3 | T6bbllslepton | 18 |
| 4 | Conclusion | 20 |

1 Introduction

In December 2015 the CMS collaboration released the results of several supersymmetry (SUSY) searches [1–7] with the first 13 TeV data. These searches found no evidence for physics beyond the Standard Model (SM). In this note we present a number of new interpretations of these experimental results in the context of SUSY simplified models (SMS). These results are based on data from pp collisions at $\sqrt{s} = 13$ TeV collected by the CMS experiment [8] during 2015, with an integrated luminosity of $2.2\text{--}2.3\text{ fb}^{-1}$.

In Section 2 we briefly describe these searches. The results are presented in Section 3 as limits at 95% confidence level (C.L.) on the production cross sections of squark and gluino pairs in the various SMS. Using the theoretical predictions for the production cross-sections of SUSY particles, these limits are then turned into constraints on the masses of SUSY particles in the different SMS scenarios.

2 Included searches

The searches considered in this note and described below are based on hadronic or leptonic final states, significant hadronic jet activity, and missing transverse energy (E_T^{miss}). All of these searches define several signal regions binned in combinations of jet multiplicity (N_{jets}), b-jet multiplicity ($N_{\text{b-jets}}$), the scalar sum of the transverse momenta of selected jets (H_T), and some measure of the E_T^{miss} , e.g., E_T^{miss} itself or H_T^{miss} , the magnitude of the vectorial sum of jet p_T .

2.1 Hadronic final states searches

This category includes the following searches :

- A search for new physics based on H_T^{miss} and requiring $N_{\text{jets}} \geq 4$ [1].
- A search for new physics with $N_{\text{jets}} \geq 1$ that uses the M_{T2} variable instead of E_T^{miss} or H_T^{miss} to reduce the QCD background [2].
- A second search with $N_{\text{jets}} \geq 1$ which uses H_T^{miss} , the dimensionless kinematic variable α_T , and very tight kinematical requirements to further reduce the QCD background [4].
- A search with $N_{\text{jets}} \geq 4$ which utilizes the Razor variables [3] to search for resonances or anomalous excesses in the distributions of those variables. The Razor search includes three event categories: an electron + multijet, a muon+multijet, and a multijet category.

2.2 Leptonic final states searches

This category includes three analyses :

- A search for new physics in events with a single lepton, $N_{\text{jets}} \geq 6$, and $N_{\text{b-jets}} \geq 1$ [5]. This analysis exploits the scalar sum of masses of large radius jets (M_{J}). For the dominant background source ($t\bar{t}$ production), this variable is largely uncorrelated with the transverse mass formed by the lepton p_T and the E_T^{miss} (M_T). This allows for a robust estimate of the background utilizing a control region characterized by low M_T .
- A search for new physics based on events with two same-sign (SS) leptons and $N_{\text{jets}} \geq 2$ [6]. Signal regions are also defined in terms of the p_T of the leptons and the

M_T^{\min} variable, defined as the minimum of the transverse mass between one of the two leptons and the E_T^{miss} . This kinematic variable reduces backgrounds from the $t\bar{t}$ process.

- A search for new physics in events with opposite-sign (OS) same-flavor leptons [7], where the search strategy depends on the invariant mass ($M_{\ell\ell}$) of the dilepton pair. If $M_{\ell\ell}$ is consistent with the Z boson mass (M_Z), the new physics hypothesis that is being tested is an excess of events at very high E_T^{miss} over the SM expectations. Conversely, if $M_{\ell\ell}$ is not consistent with M_Z , the search focusses on a possible excess of events at moderate E_T^{miss} , possibly showing the triangular shape in the $M_{\ell\ell}$ distribution characteristic of certain SUSY models.

3 New interpretations

In this section we present the new interpretations on the SMS that we consider. The models are classified according to the hard process, pair production of either gluinos or squarks, and the final decay chain. These are briefly described on the following Sections, including information on branching ratios (\mathcal{BR}) to specific final states, and on the mass splitting between the SUSY particles involved. An overview of these models can be found in Table 1. Results are presented as exclusions at 95 % C.L. on the 2D mass planes of the sparticles used to parametrize the SMS. In all exclusion figures, the thick black line delimits the observed exclusion region, whilst the thin lines show its dependence on the theoretical uncertainties on the production cross-sections. The dashed red lines indicate the expected limits as well as their expected ± 1 standard deviation variations.

Table 1: Overview of the SMS employed for the new interpretations included in this note.

| SMS | Decays | \mathcal{BR} | Notes |
|-----------------------|---|------------------|---|
| T1tttt | $\tilde{g} \rightarrow t\bar{t}\tilde{\chi}_1^0$ | 1 | - |
| T1ttbb | $\tilde{g} \rightarrow t b \tilde{\chi}^\pm, \tilde{\chi}^\pm \rightarrow W^{\pm*} \tilde{\chi}_1^0$ | 1 | $M_{\tilde{\chi}^\pm} - M_{\tilde{\chi}_1^0} = 5 \text{ GeV}$ |
| T5ttcc | $\tilde{g} \rightarrow t \tilde{t}_1, \tilde{t}_1 \rightarrow c \tilde{\chi}_1^0$ | 1 | $M_{\tilde{\chi}_1^0} - M_{\tilde{t}_1} = 20 \text{ GeV}$ |
| T5qqqqWW _A | $\tilde{g} \rightarrow \tilde{\chi}^\pm q \bar{q}, \tilde{\chi}^\pm \rightarrow W^{\pm*} \tilde{\chi}_1^0$ | 1 | $M_{\tilde{\chi}^\pm} = 0.5(M_{\tilde{g}} + M_{\tilde{\chi}_1^0})$ |
| T5qqqqWW _B | $\tilde{g} \rightarrow \tilde{\chi}^\pm q \bar{q}, \tilde{\chi}^\pm \rightarrow W^{\pm*} \tilde{\chi}_1^0$ | 1 | $M_{\tilde{\chi}^\pm} - M_{\tilde{\chi}_1^0} = 20 \text{ GeV}$ |
| T5ttttDM175 | $\tilde{g} \rightarrow \tilde{t}_1 t, \tilde{t}_1 \rightarrow t \tilde{\chi}_1^0$ | 1 | $M_{\tilde{t}_1} - M_{\tilde{\chi}_1^0} = 175 \text{ GeV}$ |
| T5ttttDegen | $\tilde{g} \rightarrow \tilde{t}_1 t, \tilde{t}_1 \rightarrow W^{\pm*} b \tilde{\chi}_1^0$ | 1 | $M_{\tilde{t}_1} - M_{\tilde{\chi}_1^0} = 20 \text{ GeV}$ |
| T2qq | $\tilde{q} \rightarrow q \tilde{\chi}_1^0$ | 1 | - |
| T2tt | $\tilde{t}_1 \rightarrow t \tilde{\chi}_1^0$ | 1 | - |
| T2bb | $\tilde{b}_1 \rightarrow b \tilde{\chi}_1^0$ | 1 | - |
| T6ttWW | $\tilde{b}_1 \rightarrow t \tilde{\chi}^\pm, \tilde{\chi}^\pm \rightarrow W^{\pm*} \tilde{\chi}_1^0$ | 1 | $M_{\tilde{\chi}_1^0} = 50 \text{ GeV}$ |
| T6bbllslepton | $\tilde{b}_1 \rightarrow b \tilde{\chi}_2^0, \tilde{\chi}_2^0 \rightarrow Z^{0*} \tilde{\chi}_1^0$ | 0.5 | $M_{\tilde{\chi}_1^0} = 100 \text{ GeV}$ $M_{\tilde{\ell}} = 0.5(M_{\tilde{\chi}_2^0} + M_{\tilde{\chi}_1^0})$ |
| | $\tilde{b}_1 \rightarrow b Z^{0*} \tilde{\chi}_2^0, \tilde{\chi}_2^0 \rightarrow \ell \tilde{\ell}, \tilde{\ell} \rightarrow \tilde{\chi}_1^0 \ell$ | 4×0.125 | $\ell = e^\pm, \mu^\pm$ |

3.1 Gluino induced decays

The core SUSY process for these models is gluino pair production with several scenarios depending on the gluino decay chain.

3.1.1 T1tttt

In this model, each \tilde{g} decays to a t quark, its anti-particle and the lightest neutralino $\tilde{\chi}_1^0$. The schematic diagram of this SMS is shown in Fig. 1.

Exclusion limits for T1tttt were already released in December 2015 for all searches considered here except for the α_T and OS searches [1–3, 5, 6]. Here we add an interpretation for the α_T search (the OS search is not sensitive to this SMS).

In this model, the α_T search excludes gluinos lighter than about 1 TeV for $\tilde{\chi}_1^0$ masses below 400 GeV, as shown in Fig. 2. The weaker-than-expected limit has been investigated, and has been attributed to a small excess of events in two adjacent bins with $N_{\text{jets}} \geq 5$, $N_{\text{b-jets}} \geq 2$, and $800 \text{ GeV} < H_T < 1000 \text{ GeV}$. These event counts are compatible with statistical fluctuations, and their effect on the T1tttt limits is enhanced on the α_T analysis compared to other analyses due to details of event selection and binning.

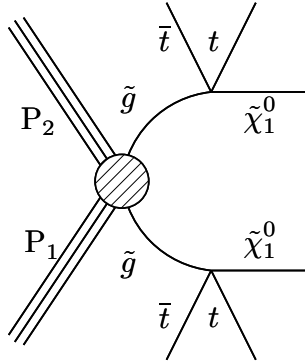


Figure 1: The T1tttt model where each \tilde{g} decays to a t quark, its anti-particle and a $\tilde{\chi}_1^0$.

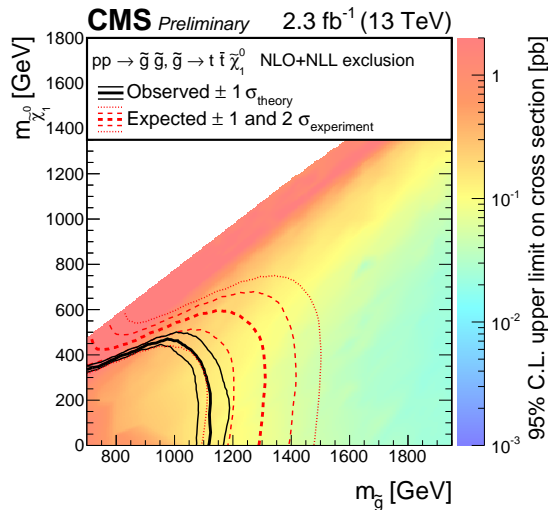


Figure 2: Upper limits and exclusion region at 95% C.L. in the \tilde{g} vs. $\tilde{\chi}_1^0$ mass plane for the T1tttt SMS set by the α_T analysis [4].

3.1.2 T5tttDM175 and T5tttDegen

Each \tilde{g} on these models decays to a t quark and its SUSY partner (\tilde{t}_1). In the case of the T5tttDM175 scenario, the \tilde{t}_1 further decays to a t quark and the $\tilde{\chi}_1^0$, with the \tilde{t}_1 having approximately the smallest mass consistent with two-body decay, i.e., $M_{\tilde{t}_1} - M_{\tilde{\chi}_1^0} = 175$ GeV. In the case of the T5tttDegen, the \tilde{t}_1 decays to a t quark and a virtual off-shell W boson giving rise to a four-body decay. In this case the mass splitting between the \tilde{t}_1 and the $\tilde{\chi}_1^0$ is chosen to be only 20 GeV. These models are illustrated in Fig. 3.

We note that these SMS result on the same final state as the T1ttt model of Section 3.1.1, but with different intermediate decay chains. These models are considered in order to test the sensitivity of our searches to T1ttt-like final states with compressed mass spectra, where the experimental acceptances are reduced.

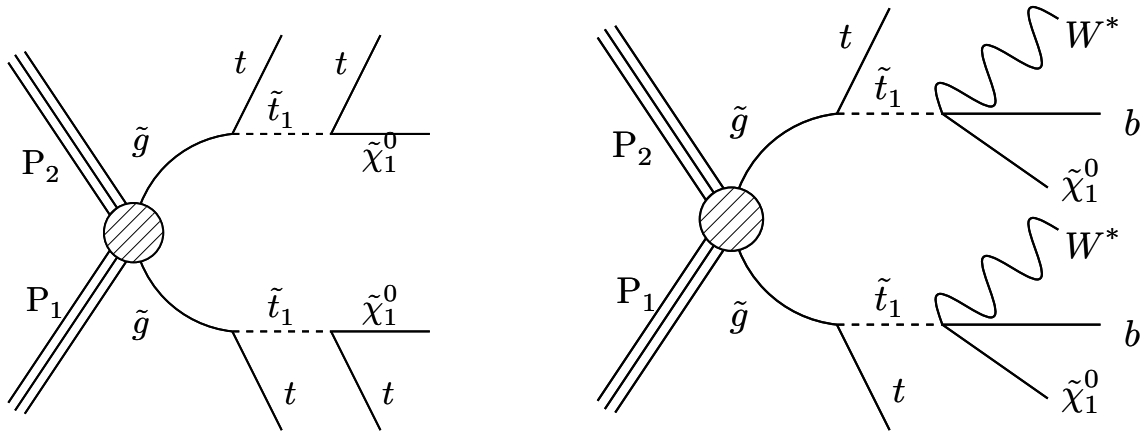


Figure 3: The T5tttDM175 model (left) where each \tilde{g} decays to a t quark and a \tilde{t}_1 , with the latter decaying to the $\tilde{\chi}_1^0$ and a t quark. The mass splitting of the \tilde{t}_1 and the $\tilde{\chi}_1^0$ is 175 GeV. In the T5tttDegen model (right) the \tilde{t}_1 decays to a bottom quark, a $\tilde{\chi}_1^0$, and a virtual W boson.

The limits from the SS dilepton analysis on the T5tttDM175 model is shown in Fig. 4, where gluinos with masses of up to around 1300 (1100) GeV when the $\tilde{\chi}_1^0$ mass is around 0 (775) GeV are excluded. These limits are very similar to those obtained by the SS dilepton search on the T1ttt model [6]. In the case of the T5tttDegen model, the SS dilepton analysis is slightly less restrictive in the \tilde{g} - $\tilde{\chi}_1^0$ mass plane, see Fig. 5. It excludes \tilde{g} with mass less than 1200 (850) GeV for a $\tilde{\chi}_1^0$ with mass around 0 (700) GeV.

The results of the single lepton search M_J are also interpreted in the T5tttDM175 model. For consistency, the signal model used in this study includes not only gluino-pair production, but also the direct production of $\tilde{t}_1\tilde{t}_1$ pairs. However, the effect of top squark pair production on the result is very small. Fig. 6 shows the excluded region in the \tilde{g} - $\tilde{\chi}_1^0$ mass plane for this combined model with both gluino-mediated top squark production and direct top squark pair production. In most of the plane, the boundary of the exclusion region is close to that obtained by this search for the T1ttt model [5]. This implies that the dependence of the \tilde{g} and the $\tilde{\chi}_1^0$ mass limits on the value of the \tilde{t}_1 mass is small. At low values of $M_{\tilde{\chi}_1^0}$ the sensitivity is reduced because the $\tilde{\chi}_1^0$ carries very little momentum in both the \tilde{t}_1 rest frame and the laboratory frame.

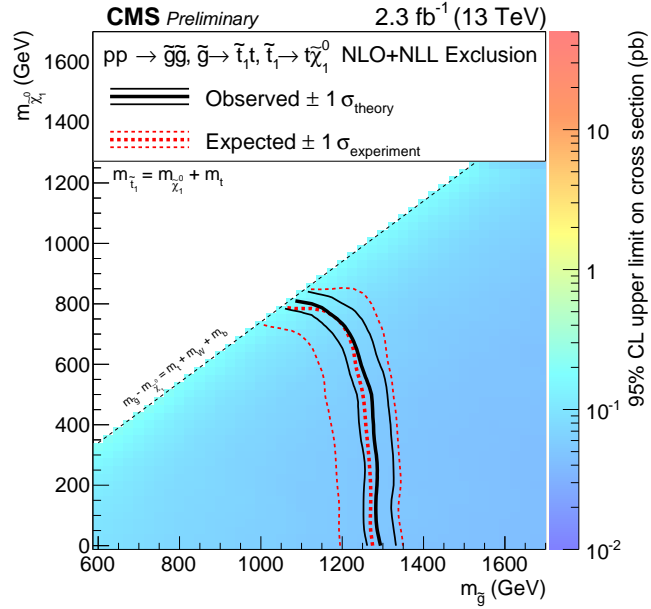


Figure 4: Upper limits and exclusion region at 95% C.L. in the \tilde{g} - $\tilde{\chi}_1^0$ mass plane for the T5tttDM175 model from the SS dilepton analysis [6].

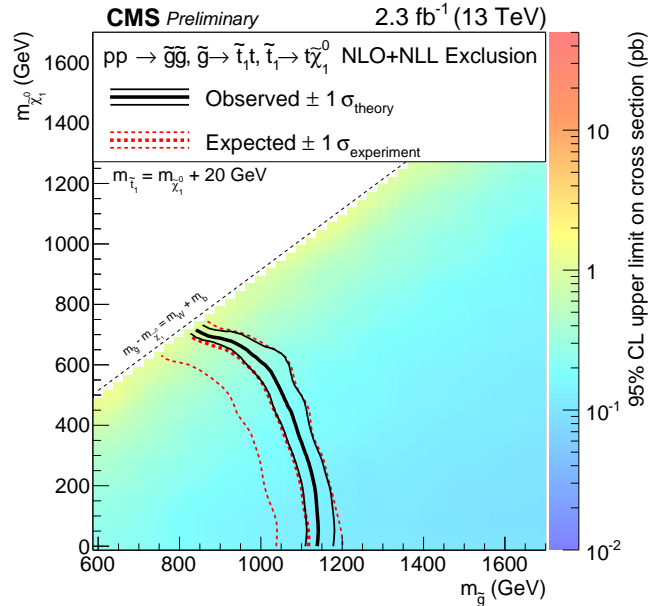


Figure 5: Upper limits and exclusion region at 95% C.L. in the \tilde{g} - $\tilde{\chi}_1^0$ mass plane for the T5tttDegen model from the SS dilepton analysis [6].

3.1.3 T1ttbb

In this scenario, each gluino decays to one of the following final states:

- The lightest chargino ($\tilde{\chi}^\pm$), a top (anti-top) and a anti-bottom (bottom) quark, with the $\tilde{\chi}^\pm$ undergoing a decay to an undetected $\tilde{\chi}_1^0$ and a virtual W boson. In this case, the mass splitting between the $\tilde{\chi}^\pm$ and the $\tilde{\chi}_1^0$ is set to 5 GeV.
- to a top or a bottom quark, its anti-particle, and a $\tilde{\chi}_1^0$.

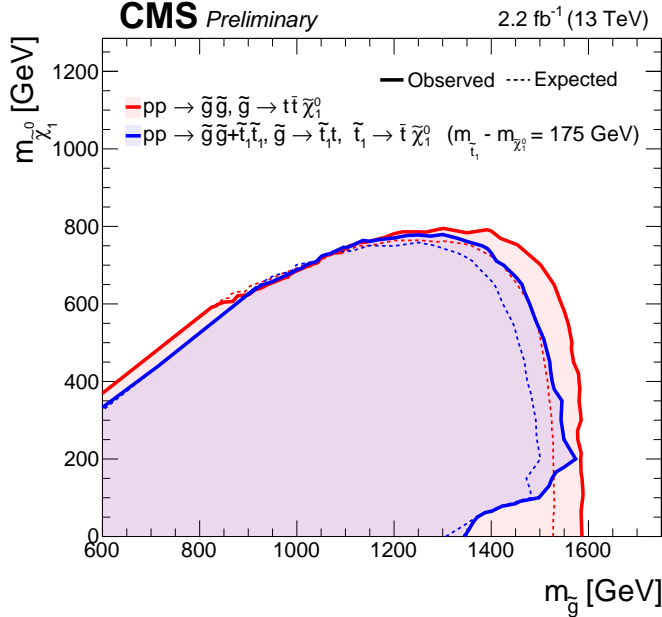


Figure 6: Exclusion region at 95% C.L. (blue) in the \tilde{g} - $\tilde{\chi}_1^0$ mass plane for a model combining gluino pair production, followed by gluino decay to an on-shell top squark, together with direct \tilde{t}_1 - \tilde{t}_1 pair production set by the single lepton search M_J [5]. The top squarks decay via the two-body process $\tilde{t}_1 \rightarrow t \tilde{\chi}_1^0$. The $\tilde{\chi}_1^0$ and \tilde{t}_1 masses are related by the constraint $M_{\tilde{t}_1} = M_{\tilde{\chi}_1^0} + 175$ GeV. For comparison, the exclusion region at 95% C.L. for the T1tttt model, which has three-body gluino decay (red) is overlaid.

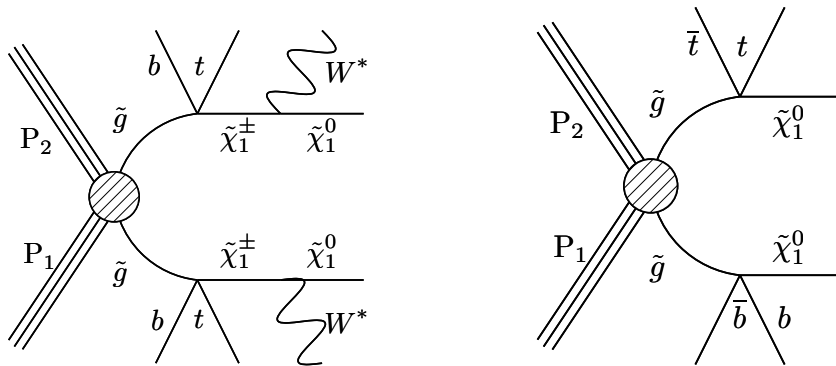


Figure 7: The T1ttbb model with two out of its six possible topologies.

Two of the six possible topologies are shown in Fig. 7.

We consider the following set of branching ratios:

- $\mathcal{BR} = 100\%$ for $\tilde{g} \rightarrow b \bar{b} \tilde{\chi}_1^0$
- $\mathcal{BR} = 50\%$ for $\tilde{g} \rightarrow t b \tilde{\chi}_1^\pm$ and $\mathcal{BR} = 50\%$ for $\tilde{g} \rightarrow b \bar{b} \tilde{\chi}_1^0$
- $\mathcal{BR} = 100\%$ for $\tilde{g} \rightarrow t b \tilde{\chi}_1^\pm$
- $\mathcal{BR} = 50\%$ for $\tilde{g} \rightarrow t b \tilde{\chi}_1^\pm$, $\mathcal{BR} = 25\%$ for $\tilde{g} \rightarrow t \bar{t} \tilde{\chi}_1^0$, $\mathcal{BR} = 25\%$ for $\tilde{g} \rightarrow b \bar{b} \tilde{\chi}_1^0$
- $\mathcal{BR} = 50\%$ for $\tilde{g} \rightarrow t b \tilde{\chi}_1^\pm$, $\mathcal{BR} = 50\%$ for $\tilde{g} \rightarrow t \bar{t} \tilde{\chi}_1^0$
- $\mathcal{BR} = 100\%$ for $\tilde{g} \rightarrow t \bar{t} \tilde{\chi}_1^0$ (this the T1tttt SMS of Section 3.1.1).

Fig. 8-9 show the expected and observed exclusion contours in the \tilde{g} - $\tilde{\chi}_1^0$ mass plane, for different branching ratio choices, from the all hadronic multijets + H_T^{miss} and from the Razor analyses respectively. In addition, Fig. 10 the limits from the multijets + H_T^{miss} analysis are shown for $\mathcal{BR}(\tilde{g} \rightarrow t b \tilde{\chi}^\pm) = 100\%$, and Fig. 11 presents limits from the Razor analysis for a more generic case where at each point in the \tilde{g} - $\tilde{\chi}_1^0$ mass plane the $\mathcal{BR}(\tilde{g} \rightarrow t b \tilde{\chi}^\pm)$ is chosen in such a way as to yield the largest expected cross section upper limit, i.e., the worst-case expected exclusion. This then gives a \mathcal{BR} -independent conservative exclusion.

We find that the exclusion curves are fairly independent of \mathcal{BR} , except in the case of $\mathcal{BR}(\tilde{g} \rightarrow t b \tilde{\chi}^\pm) = 100\%$ and very low $\tilde{\chi}_1^0$ mass, where the sensitivity is reduced.

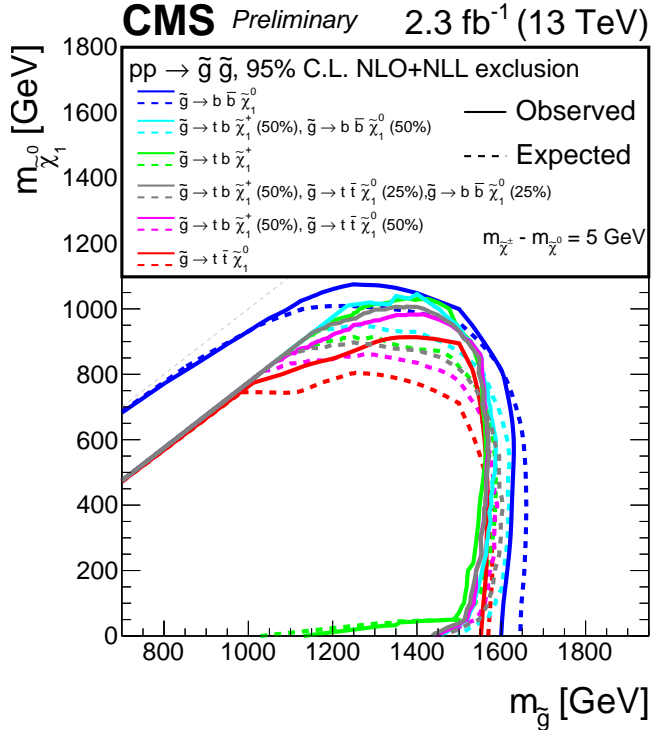


Figure 8: Exclusion region in the \tilde{g} - $\tilde{\chi}_1^0$ mass plane at 95% C.L., for \tilde{g} pair production on the T1ttbb SMS for different choices of the \tilde{g} branching ratio into top and bottom quarks set by the multijets + H_T^{miss} analysis [1].

The results of the SS dilepton search are also used to constrain this model for $\mathcal{BR}(\tilde{g} \rightarrow t b \tilde{\chi}^\pm) = 100\%$ (Fig. 12). Here \tilde{g} masses up to about 1250 (1000) GeV for $\tilde{\chi}_1^0$ mass of 0 (700) GeV are excluded.

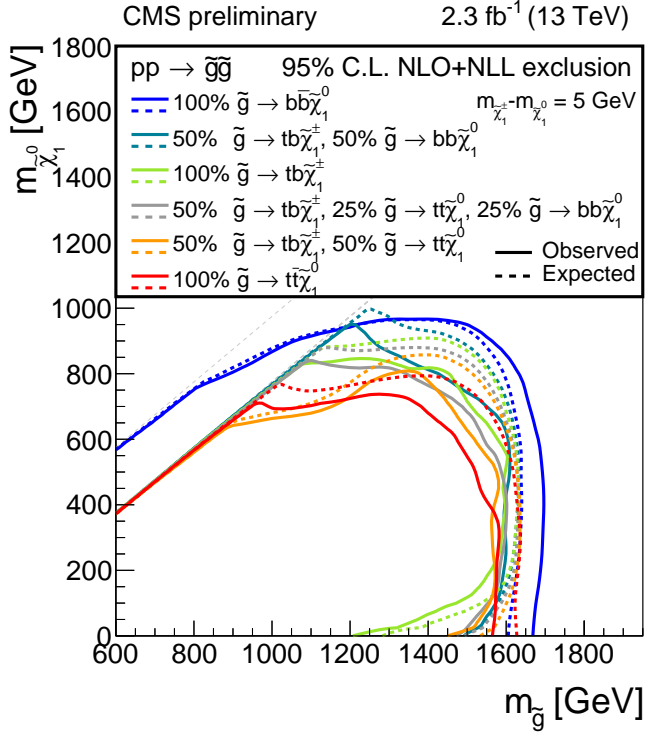


Figure 9: Exclusion region in the \tilde{g} - $\tilde{\chi}_1^0$ mass plane at 95% C.L., for \tilde{g} pair production on the T1ttbb SMS for different choices of the \tilde{g} branching ratio into top and bottom quarks set by the Razor analysis [3].

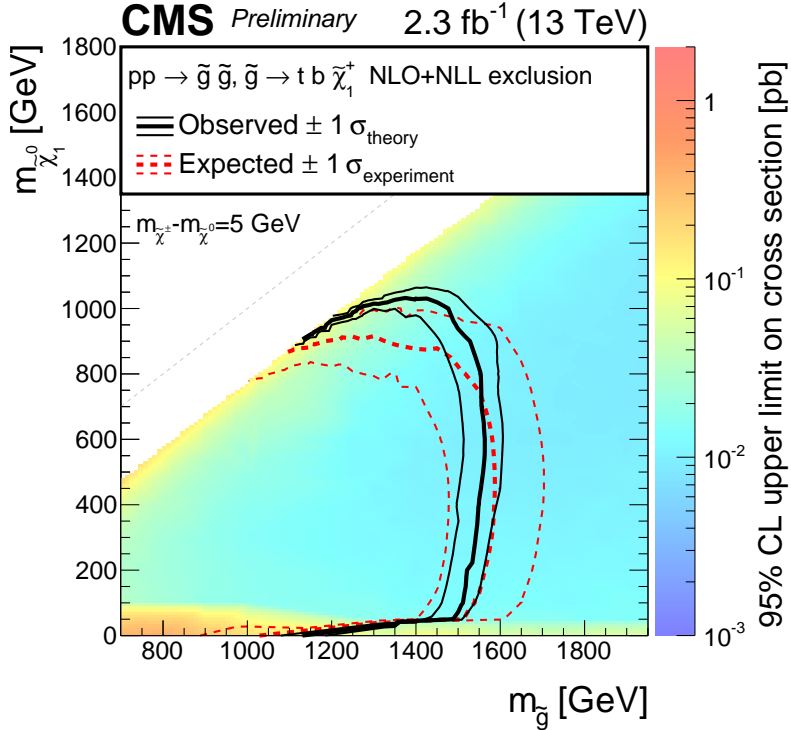


Figure 10: Upper limits and exclusion region in the \tilde{g} - $\tilde{\chi}_1^0$ mass plane at 95% C.L., obtained for \tilde{g} pair production on the T1ttbb SMS for $\mathcal{BR}(\tilde{g} \rightarrow tb\tilde{\chi}_1^\pm) = 100\%$ set by the all hadronic multijets + H_T^{miss} analysis [1].

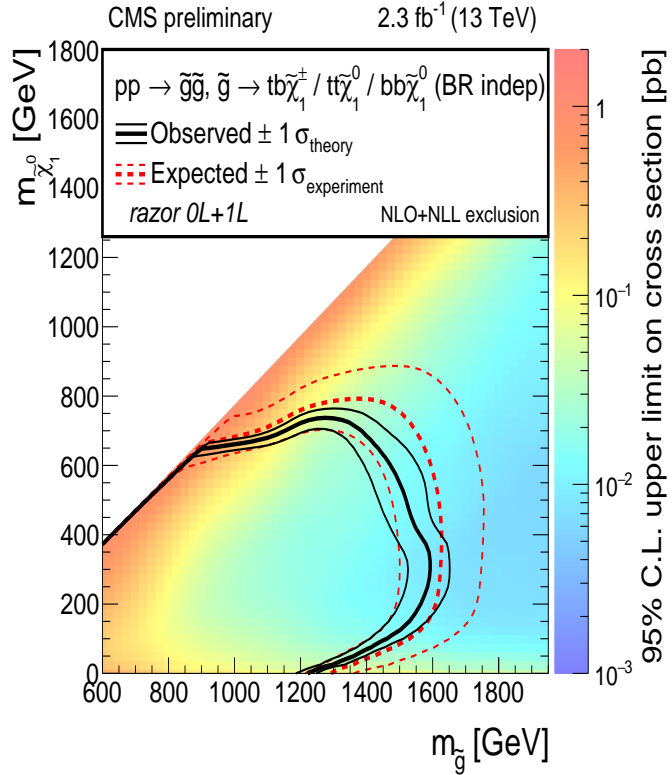


Figure 11: Upper limits and exclusion region in the \tilde{g} - $\tilde{\chi}_1^0$ mass plane at 95% C.L., obtained for \tilde{g} pair production on the T1ttbb SMS for $\mathcal{BR}(\tilde{g} \rightarrow t b \tilde{\chi}_1^\pm) = 100\%$ set by the Razor analysis [3].

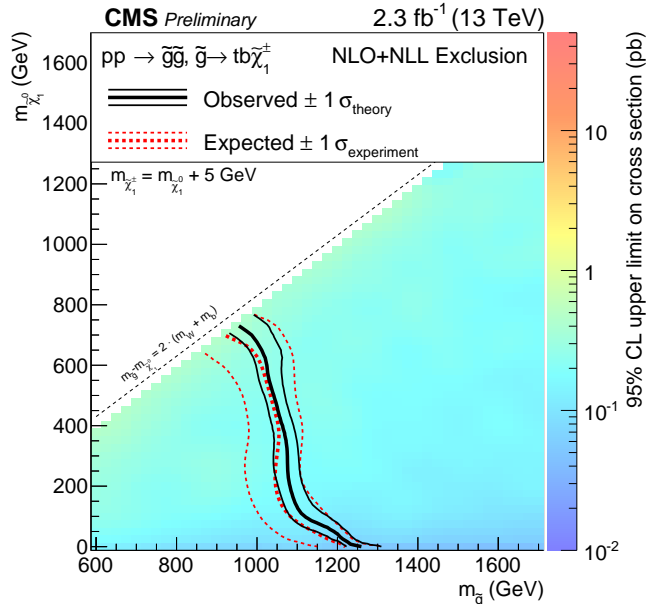


Figure 12: Upper limits and exclusion region at 95% C.L. in the \tilde{g} - $\tilde{\chi}_1^0$ mass plane at 95% C.L. for the T1ttbb SMS or $\mathcal{BR}(\tilde{g} \rightarrow t b \tilde{\chi}_1^\pm) = 100\%$ set by the SS dilepton analysis [6].

3.1.4 T5ttcc

In this model, each gluino decays to a stop squark and an anti-top quark or their charge conjugates with equal probability. The top squark (anti-squark) decays to a c quark (anti-quark) and a $\tilde{\chi}_1^0$. The mass difference between the \tilde{t}_1 and the $\tilde{\chi}_1^0$ is chosen to have the small value of 20 GeV. The schematic diagram of this model is given in Fig. 13.

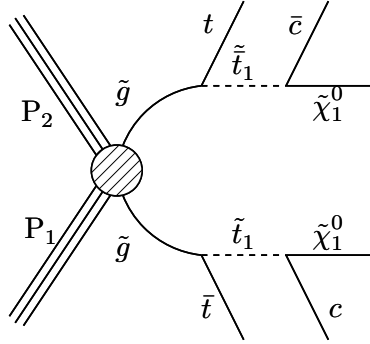


Figure 13: The T5ttcc model where each \tilde{g} decays to a \tilde{t}_1 ($\tilde{\bar{t}}_1$) and a \bar{t} (t quark), with the \tilde{t}_1 ($\tilde{\bar{t}}_1$) cascading to a $\tilde{\chi}_1^0$ and a c (\bar{c}) quark.

The SS dilepton search sets upper limits in the \tilde{g} - $\tilde{\chi}_1^0$ mass plane as shown in Fig. 14. The gluino mass limit is about 1050 GeV for $\tilde{\chi}_1^0$ mass up to about 600 GeV. For even higher $\tilde{\chi}_1^0$ masses, the gluino limit is reduced by as much as 200 GeV. These limits are not as stringent as those obtained by interpreting the same experimental results on the context of the T1tttt model [6], since there are fewer leptons in T5ttcc than in T1tttt.

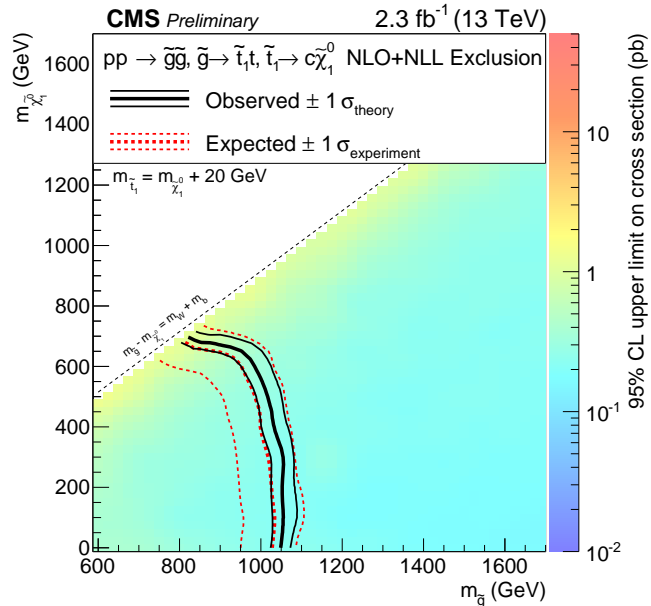


Figure 14: Upper limits and exclusion region at 95% C.L. in the \tilde{g} - $\tilde{\chi}_1^0$ mass plane at 95% C.L. for the T5ttcc SMS set by the SS dilepton analysis [6].

3.1.5 T5qqqqWW

In this scenario each \tilde{g} decays to a $\tilde{\chi}^\pm$ and a pair of first or second generation SM quarks. The $\tilde{\chi}^\pm$ further decays to a $\tilde{\chi}_1^0$ and a W boson. Consequently, the final state consists of the decay products of the virtual W boson, four quarks, and two $\tilde{\chi}_1^0$'s. The schematic diagram of this model is depicted in Fig. 15.

We consider the following two configuration:

- Model A, where the $\tilde{\chi}^\pm$ has a mass equal to the median of the $\tilde{\chi}_1^0$ and the \tilde{g} mass;
- Model B, where the mass splitting between the $\tilde{\chi}^\pm$ and the $\tilde{\chi}_1^0$ is 20 GeV.

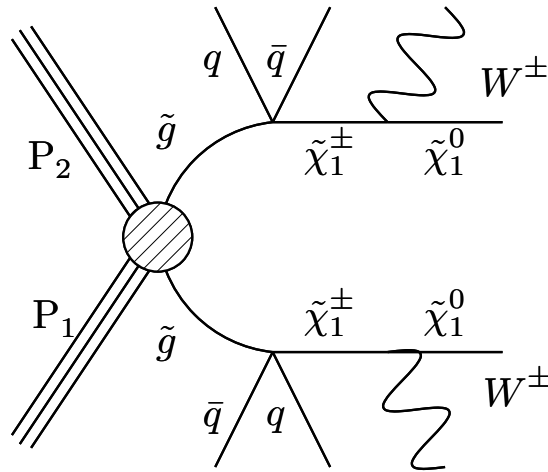


Figure 15: The T5qqqqWW model where each \tilde{g} decays to a $\tilde{\chi}^\pm$ and pair of quarks of the first or the second generation. The $\tilde{\chi}^\pm$ further decays to a $\tilde{\chi}_1^0$ and a virtual W boson.

The results of the SS dilepton analysis are used to set exclusion limits for these two models. For model A we exclude gluinos lighter than 1.1 TeV for $\tilde{\chi}_1^0$ lighter than 600 GeV (Fig. 16). For model B, \tilde{g} lighter than about 1000 (500) GeV are excluded for a $\tilde{\chi}_1^0$ with mass around 0 (600) GeV (Fig. 17).

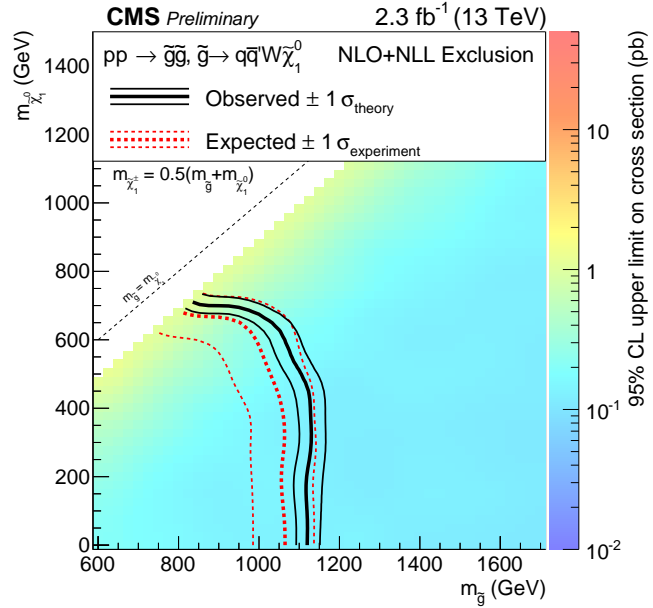


Figure 16: Upper limits and exclusion region at 95% C.L. in the \tilde{g} vs. $\tilde{\chi}_1^0$ mass plane for the T5qqqqWW model when $M_{\tilde{\chi}^\pm} = 0.5(M_{\tilde{g}} + M_{\tilde{\chi}_1^0})$ set by the SS dilepton search [6].

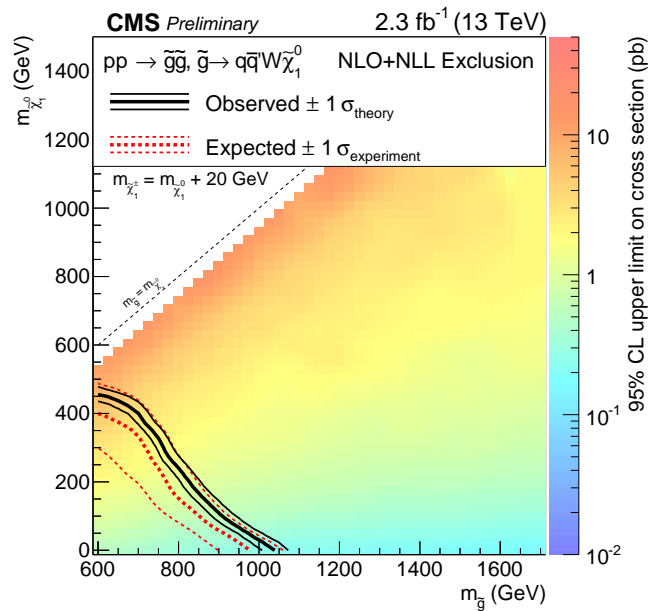


Figure 17: Upper limits and exclusion region at 95% C.L. in the \tilde{g} vs. $\tilde{\chi}_1^0$ mass plane for the T5qqqqWW model when $\Delta(M_{\tilde{\chi}^\pm} - M_{\tilde{\chi}_1^0}) = 20$ GeV set by the SS dilepton search [6].

3.2 Squark induced decays

The basic SUSY process for these models is squark pair production.

3.2.1 T2qq, T2tt, T2bb

In the T2qq model, a pair of first or second generation squarks is produced, each one decaying to a SM quark and a $\tilde{\chi}_1^0$. For the T2tt and T2bb models, a top (bottom) squark and its anti-particle is produced decaying to a top (bottom) SM quark and a $\tilde{\chi}_1^0$. For the T2tt model, depending on the mass splitting between the \tilde{t}_1 and the $\tilde{\chi}_1^0$, the former can undergo either two, three or four-body decays. These models are shown in Fig. 18. The results of the M_{T2} and the multijet + H_T^{miss} analyses are interpreted on these SMS as shown in Fig. 19-22.

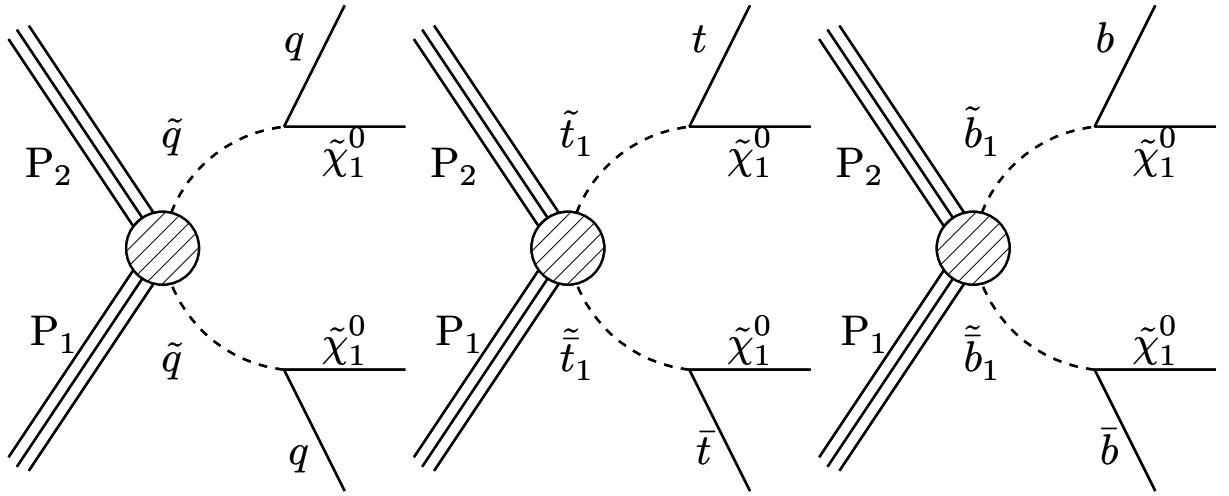


Figure 18: The T2qq (left) T2tt (middle) and the T2bb (right) SMS models. For the T2qq a pair of first or second generation squarks is produced decaying to a pair of quarks and two $\tilde{\chi}_1^0$. For the T2tt (T2bb) models, a pair of top (bottom) squark and its anti-particle is produced which decay to a top (bottom) quark/antiquark and a $\tilde{\chi}_1^0$.

More specifically, for T2qq, the M_{T2} analysis probes squark masses up to around 1250 GeV for $\tilde{\chi}_1^0$ masses around 580 GeV, when the first and second generation squarks are considered. When only one light squark is considered, the exclusion limits only reach up to squark masses of 600 GeV for masses up to 300 GeV for the $\tilde{\chi}_1^0$.

For the T2bb model, the M_{T2} search excludes \tilde{b}_1 masses up to 900 (775) GeV for a $\tilde{\chi}_1^0$ mass around 0 (350) GeV. The limits are shown in Fig. 20.

The results from both analyses are used to set comparable exclusion contours for the T2tt model (Fig. 21 and Fig. 22). We probe top squark masses below 750-800 GeV for massless $\tilde{\chi}_1^0$, while also excluding top squarks of masses up to about 600 GeV when the $\tilde{\chi}_1^0$ has a mass below 300 GeV. The region where $M_{\tilde{t}_1} \approx M_t + M_{\tilde{\chi}_1^0}$ is masked, as this region is particularly challenging and will be targeted by a dedicated analysis.

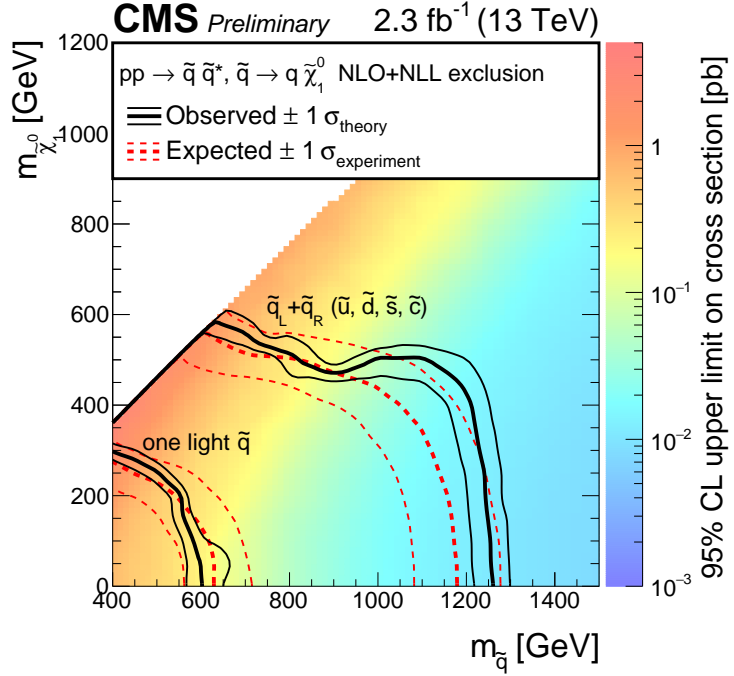


Figure 19: Upper limits and exclusion region at 95% C.L. on the \tilde{q} vs. $\tilde{\chi}_1^0$ mass plane for the T2qq SMS. Two cases are presented, one when the squarks can be any of $\tilde{u}, \tilde{d}, \tilde{c}$, or \tilde{s} , and one when only one light squark is considered. In the latter case, the limits are weaker due to the smaller production cross section. These limits are from the M_{T2} search [2].

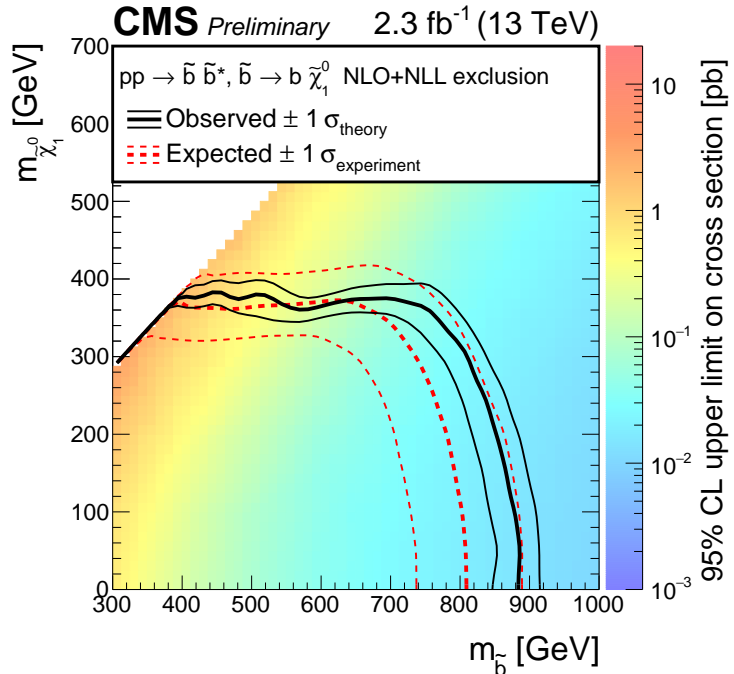


Figure 20: Upper limits and exclusion region at 95% C.L. on \tilde{b}_1 vs. $\tilde{\chi}_1^0$ mass plane for the T2bb SMS set by the M_{T2} analysis [2].

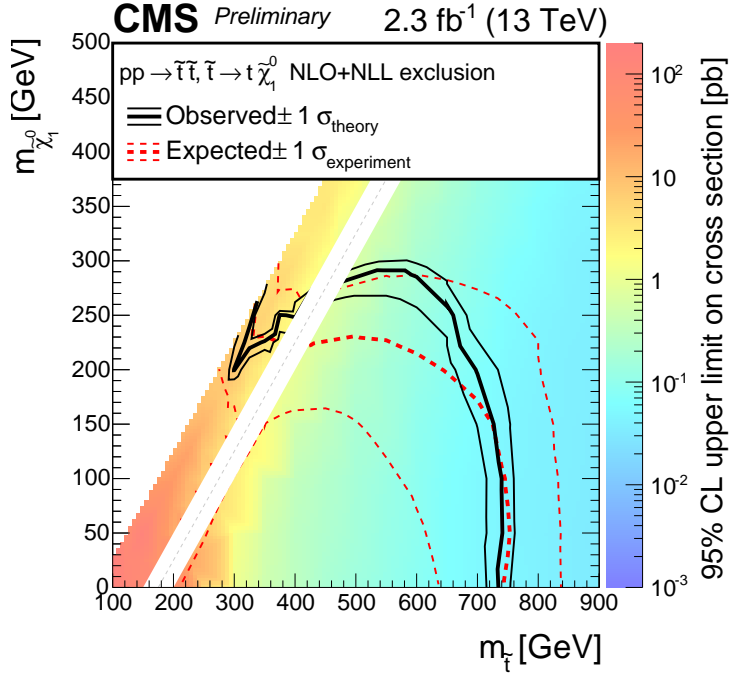


Figure 21: Upper limits and exclusion region at 95% C.L. on the \tilde{t}_1 vs. $\tilde{\chi}_1^0$ mass plane for the T2tt SMS set by the hadronic multijets + H_T^{miss} search [1]. The region where $M_{\tilde{t}_1} \approx M_t + M_{\tilde{\chi}_1^0}$ is masked, as this region of parameter space will be targeted by a dedicated analysis.

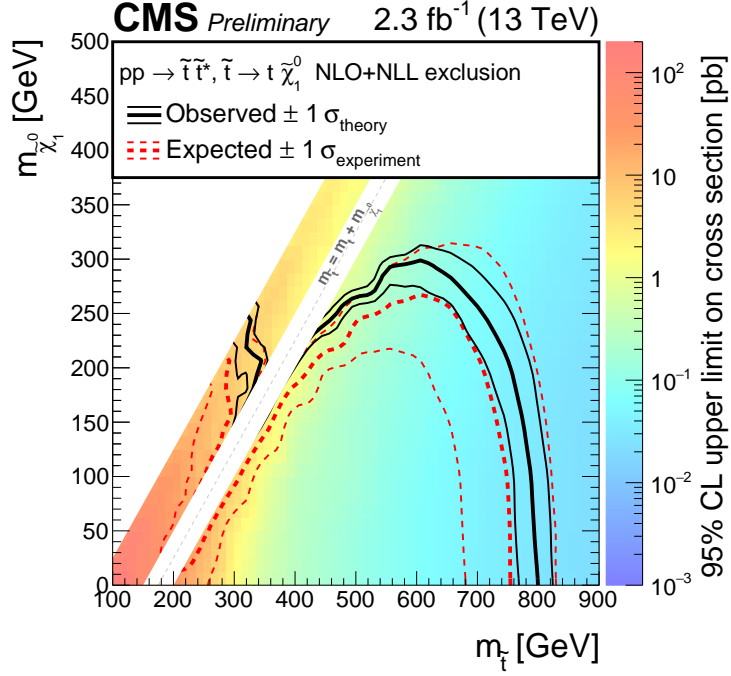


Figure 22: Upper limits and exclusion region at 95% C.L. on the \tilde{t}_1 vs. $\tilde{\chi}_1^0$ for the T2tt SMS set by M_{T2} search [2]. The region where $M_{\tilde{t}_1} \approx M_t + M_{\tilde{\chi}_1^0}$ is masked, as this region of parameter space will be targeted by a dedicated analysis.

3.2.2 T6ttWW

This model is similar to the T2bb but with different decays of the produced \tilde{b}_1 - \tilde{b}_1 pair. More specifically, each \tilde{b}_1 (\tilde{b}_1) decays to a $t(\bar{t})$ quark and a $\tilde{\chi}^\pm$. Further, and depending on the mass difference between the bottom squark and the t quark, the latter can be either on or off-shell. Finally, the $\tilde{\chi}^\pm$ decays to a virtual W boson and a $\tilde{\chi}_1^0$ with mass of 50 GeV. The model is illustrated in Fig. 23.

In Fig. 24 we show the exclusion limits at 95% C.L. set by the SS dilepton analysis, where we exclude bottom squarks lighter than about 650 GeV for $\tilde{\chi}_1^0$ masses up to around 500 GeV.

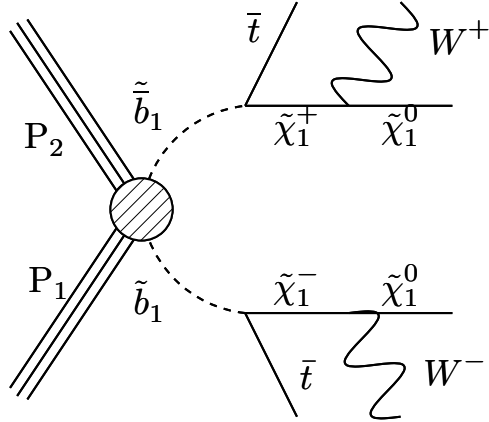


Figure 23: The T6ttWW model where each bottom squark decays to a top quark and a $\tilde{\chi}^\pm$. The $\tilde{\chi}^\pm$ further decays to a virtual W boson and a $\tilde{\chi}_1^0$ with mass of 50 GeV.

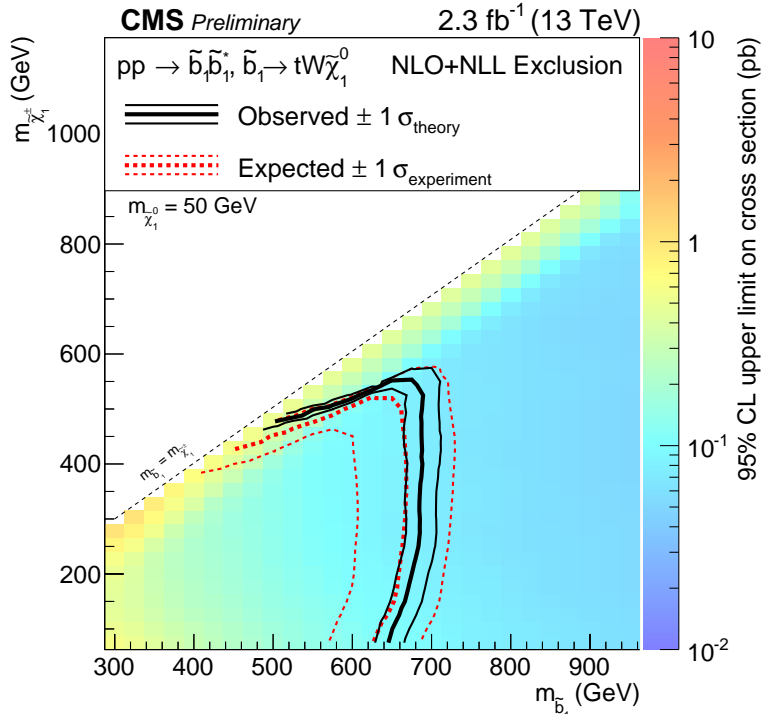


Figure 24: Upper limits and exclusion region at 95% C.L. on the \tilde{b}_1 - $\tilde{\chi}_1^0$ mass plane for the T6ttWW SMSset by the SS dilepton analysis [6].

3.2.3 T6bbllslepton

In this model, the \tilde{b}_1 decays to a $\tilde{\chi}_2^0$ and a bottom quark. The $\tilde{\chi}_2^0$ can decay to a Z boson and a $\tilde{\chi}_1^0$ with $\mathcal{BR} = 50\%$, or to a $\tilde{\ell}_L$ or a $\tilde{\ell}_R$ and a ℓ with $\mathcal{BR} = 12.5\%$ for each possible decay, with $\ell = e^\pm, \mu^\pm$. This model assumes a mass for the $\tilde{\chi}_1^0$ of 100 GeV whilst the mass of the sleptons is set to be the average of the $\tilde{\chi}_2^0$ and the $\tilde{\chi}_1^0$ masses. This model is shown in Fig. 25.

In Fig. 26 we display the exclusion limits at 95% C.L. set by the OS leptonic analysis on the \tilde{b}_1 - $\tilde{\chi}_2^0$ mass plane. Masses of \tilde{b}_1 less than about 600 GeV are excluded for $\tilde{\chi}_2^0$ masses less than about 550 GeV.

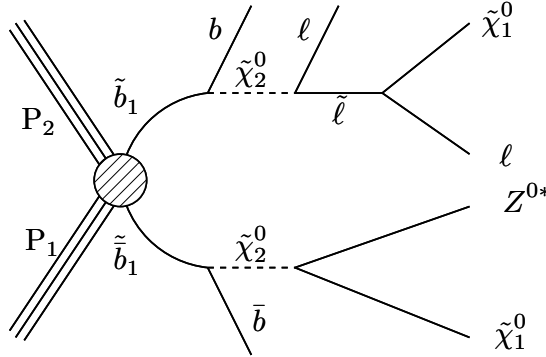


Figure 25: The T6bbllslepton model where each bottom squark decays to a $\tilde{\chi}_2^0$ and a bottom quark. The $\tilde{\chi}_2^0$ decays to a Z boson and a $\tilde{\chi}_1^0$ with a $\mathcal{BR} = 50\%$, or to a $\tilde{\ell}_L$ or a $\tilde{\ell}_R$ and a ℓ with $\mathcal{BR} = 12.5\%$ for each possible decay, with $\ell = e^\pm, \mu^\pm$.

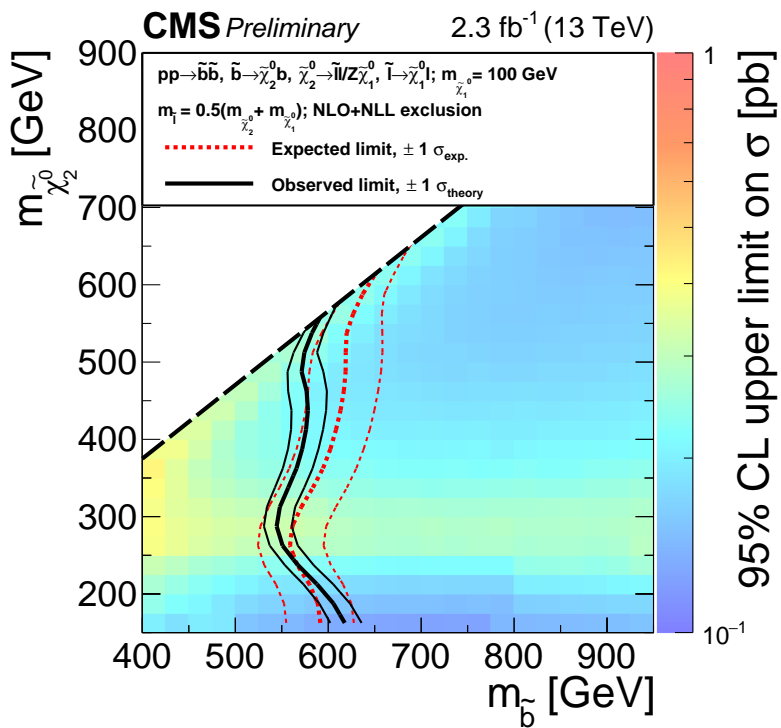


Figure 26: Upper limits and exclusion region at 95% C.L. on the \tilde{b}_1 - $\tilde{\chi}_2^0$ mass plane set by the OS leptonic analysis [7].

4 Conclusion

In this note we presented a number of new interpretations in different SUSY simplified model topologies. These results complement the previous preliminary results for searches for SUSY carried out by the CMS collaboration using data from the 2015 pp run from the LHC. Several new exclusion limits have been set, further constraining SUSY models.

References

- [1] CMS Collaboration Collaboration, "Search for supersymmetry in the multijet and missing transverse momentum channel in pp collisions at 13 TeV", Technical Report CMS-PAS-SUS-15-002, CERN, Geneva, 2015.
- [2] CMS Collaboration Collaboration, "Search for new physics in the all-hadronic final state with the MT2 variable", Technical Report CMS-PAS-SUS-15-003, CERN, Geneva, 2015.
- [3] CMS Collaboration Collaboration, "Inclusive search for supersymmetry using the razor variables at $\sqrt{s} = 13$ TeV", Technical Report CMS-PAS-SUS-15-004, CERN, Geneva, 2015.
- [4] CMS Collaboration Collaboration, "Search for new physics in final states with jets and missing transverse momentum in $\sqrt{s} = 13$ TeV pp collisions with the α_T variable", Technical Report CMS-PAS-SUS-15-005, CERN, Geneva, 2015.
- [5] CMS Collaboration Collaboration, "Search for supersymmetry in pp collisions at $\sqrt{s} = 13$ TeV in the single-lepton final state using the sum of masses of large radius jets", Technical Report CMS-PAS-SUS-15-007, CERN, Geneva, 2015.
- [6] CMS Collaboration Collaboration, "Search for SUSY in same-sign dilepton events at $\sqrt{s}=13$ TeV", Technical Report CMS-PAS-SUS-15-008, CERN, Geneva, 2015.
- [7] CMS Collaboration Collaboration, "Search for new physics in final states with two opposite-sign same-flavor leptons, jets and missing transverse momentum in pp collisions at $\sqrt{s}=13$ TeV", Technical Report CMS-PAS-SUS-15-011, CERN, Geneva, 2015.
- [8] CMS Collaboration, "The CMS experiment at the CERN LHC", *JINST* **3** (2008) S08004, doi:10.1088/1748-0221/3/08/S08004.